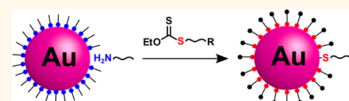


Thiolate-Protected Nanoparticles *via* Organic Xanthates: Mechanism and Implications

Volodymyr Sashuk*

Institute of Physical Chemistry, Polish Academy of Sciences, Kasprzaka 44/52, 01-224 Warsaw, Poland

ABSTRACT The gold nanoparticles (AuNPs) stabilized with amine ligands are converted into robust thiolate-protected AuNPs in the presence of xanthates. This enables decoration of the AuNPs with a diversity of important functional groups, in particular, to introduce the thiol-sensitive unsaturated C—C bonds. The ^1H NMR study on the reaction mechanism provides a new insight into the great mystery of nanoscience—the fate of hydrogen upon the formation of the Au—S bond.



KEYWORDS: gold nanoparticles · quantum dots · xanthates · thiolate-protected monolayer · self-assembly · thiol-sensitive group · fate of hydrogen

A gold–thiolate bonding is one of the fundamentals of nanoscience.^{1–3} The attachment of a functional ligand to a surface *via* a covalent gold–sulfur bond has enormous significance in view of gold nanoparticle (AuNP) applications in many nano(bio)technology fields.^{4–6} The thiolate bonding is routinely afforded in the reaction of a gold surface atom with a thiol (RSH), although a few alternative methods are also known.^{7–9} Herein, we explored a novel route to attach the ligand to the AuNP surface with no use of thiol.

We found that organic xanthates (RSC(S)OEt), when directly mixed with amine-capped AuNPs, assemble as thiolates on the NP surface. The study on the reaction mechanism provided new insights and solutions for two major issues of thiol–gold surface chemistry. *The first* issue concerns the incompatibility of thiol with many important functional groups. An enhanced nucleophilicity of the SH group, especially in basic conditions, makes the synthesis of a wide range of functionalized thiol molecules impossible and hence excludes their use in NP modification. The incompatibility problem can be overcome by protecting a functional group¹⁰ that, however, is not convenient or even applicable as in case of unsaturated C—C bonds. Here, by employing the xanthate approach, we were able to dress AuNPs with ligands containing thiol-sensitive olefin and acetylene functional groups. *The second*

issue is the fate of hydrogen upon chemisorption of thiol to the gold surface—the fundamental issue of gold–thiol interaction, which has puzzled scientists for more than two decades. The scission of the S—H bond is widely believed to proceed with evolution of molecular (or atomic) hydrogen that recently was confirmed experimentally.^{11–13} We discovered an alternative mode for the hydrogen loss and demonstrated that in the reaction of thiol with amine-capped AuNPs the hydrogen releases as a proton.

RESULTS AND DISCUSSION

In our studies, we used dodecylamine (DDA)-capped AuNPs with a core size about 5 nm prepared according to the procedure by Jana *et al.*¹⁴ The AuNPs obtained by this method have recently proved to be a versatile “stock” for on-demand functionalization allowing preparation of the mono- and mixed ligand shell AuNPs with precisely controlled chemical composition and interfacial/solvation properties.^{15–17} The organic xanthates were readily obtained from corresponding organic bromides or mesylates in reaction with potassium ethyl xanthate, which is a cheap flotation agent. Importantly, the preparation of xanthate requires one step less than the synthesis of the respective thiol.

In a typical experiment, the xanthate ligand was added to the dispersion containing amine-capped AuNPs and the mixture was left stirring for 24 h. The resulting NPs, if

* Address correspondence to vsashuk@ichf.edu.pl.

Received for review September 13, 2012 and accepted November 19, 2012.

Published online November 19, 2012
10.1021/nn304229r

© 2012 American Chemical Society

needed, were precipitated with a suitable solvent, next collected by centrifugation, and finally purified using a redispersion–precipitation technique. Following this procedure, we introduced into the AuNP ligand shell a variety of functional groups differing by solvation properties (Figure 1). For more details on the experimental procedure, see the Supporting Information.

The information on structure and chemical composition of the resulting NPs was acquired using ^1H NMR and XPS spectroscopy methods. The analyses were

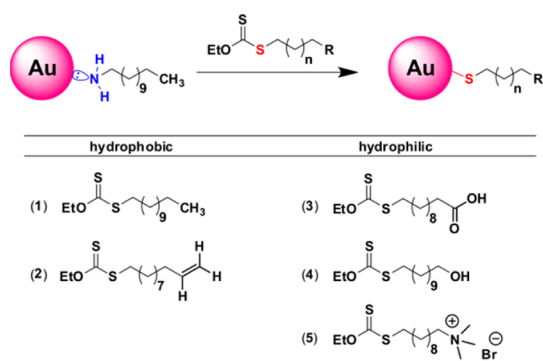


Figure 1. Schematic illustration for the preparation of thiolate-protected AuNPs using amine-capped NPs and organic xanthates with hydrophobic and hydrophilic termini.

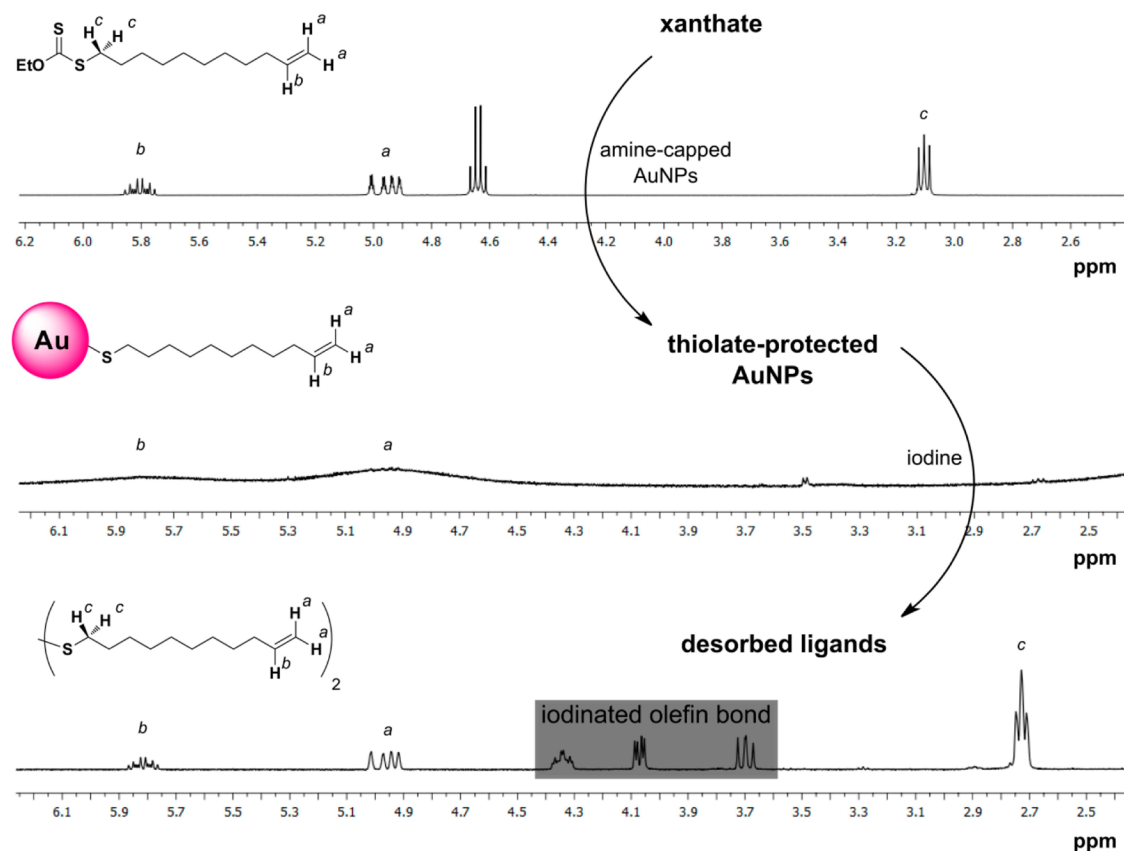


Figure 2. NMR evidence for the formation of thiolate assembly on the AuNP surface. Xanthate 2 reacts with amine-capped AuNPs, yielding the thiolate-protected NPs which contain the vinyl groups in their ligand shell. The presence of gold–thiolate bonding was confirmed by treatment of resulting NPs with iodine that led to desorption of ligands and appearance of resonance at 2.73 ppm corresponding to the disulfide bond. The formation of disulfides upon desorption from the NP surface is a characteristic feature of the thiolate ligands.

performed on the AuNPs obtained from vinyl xanthate **2**, as the prepared NPs appeared the most suitable for the NMR experiments. The NMR study is schematically presented in Figure 2. The ^1H NMR spectrum of the selected NPs, dispersed in CDCl_3 , exhibited a broadened structure (which is common for gold colloids) where only the resonances from vinyl protons can be clearly recognized. The addition of iodine to the analyzed dispersion led to desorption of the ligands from the NP surface, which facilitated reading out the NMR information. After the release of the ligands into the solution, the NMR spectral profile was narrowed and augmented in new signals. The resonances in the 3–6 ppm region are attributed to an intact and iodinated olefin bond. A triplet at 2.73 ppm corresponds to protons of the methylene group adjacent to the S–S bond, that is, to the disulfide group. The conversion to disulfides is a well-known property of thiolate ligands desorbing from the AuNP surface and serves as a quick indicator to the presence of gold–thiolate bonding. Nevertheless, the most precise information on the nature of ligand–gold bonding was drawn by comparing the XPS spectra of the AuNPs derived from the xanthate **2** and its thiol analogue (Figure 3). The XPS analysis revealed that the product of xanthate assembly resembled

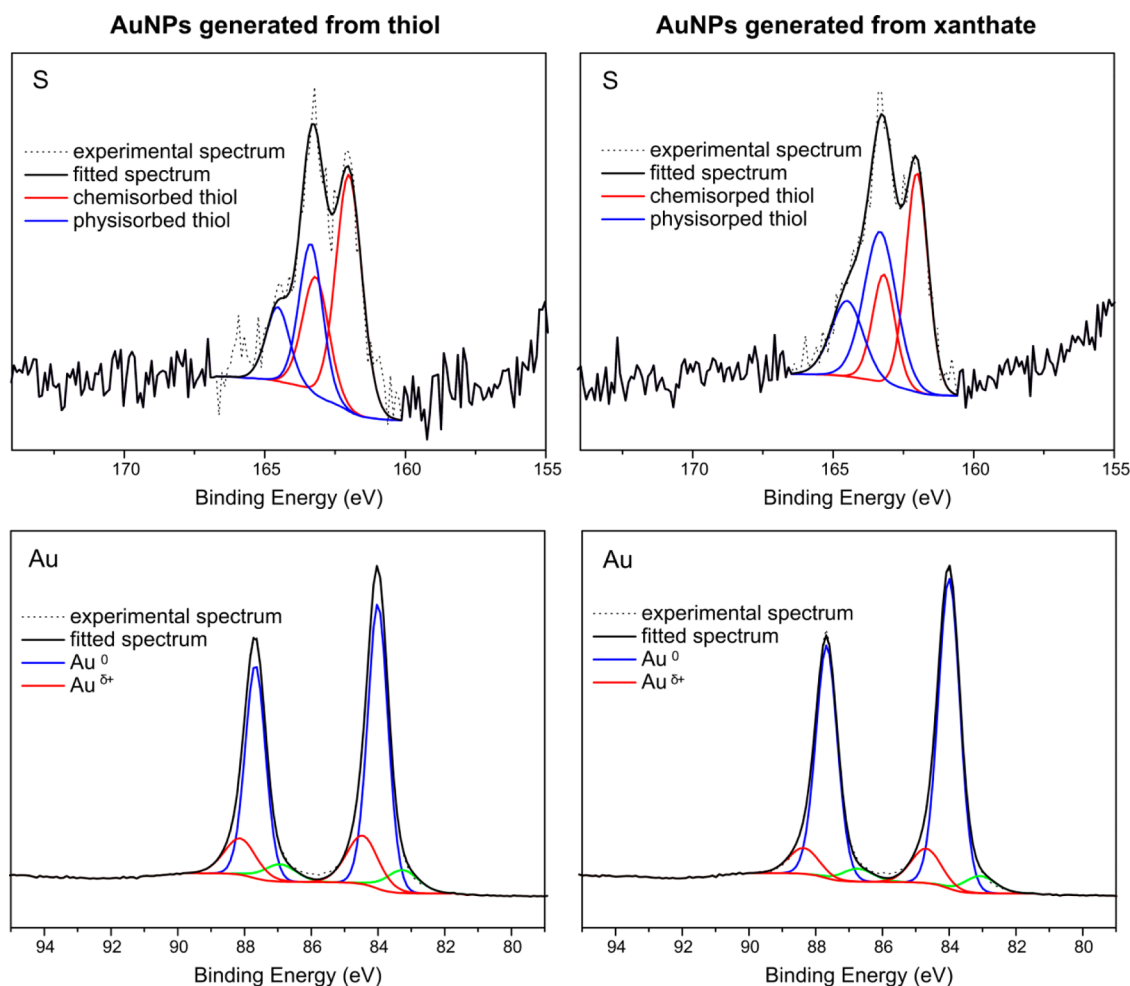


Figure 3. XPS evidence for the formation of thiolate assembly on the NP surface. The spectra represent the S2p and Au4f regions for NPs generated from xanthate 2 and the corresponding thiol analogue. The experimental and fitted data are depicted as dotted and solid lines, respectively. Binding energies were set relative to the Au4f peak (84.0 eV). For both samples, in the S2p region, the sulfur signal consists of two components which correspond to chemisorbed and physisorbed thiol. The formation of the Au–S bond is also confirmed by the presence of oxidized gold species ($\text{Au}^{\delta+}$) in the Au4f region.

that obtained from the thiol. The S2p region for both samples shows the sulfur signal composed of two components with identical binding energies and similar intensities. Each component consists of a doublet with a peak width of 1.2 eV and the peak area ratio of 1:2. The $\text{S}2\text{p}_{3/2}$ band with binding energy of 162.0 eV corresponds to chemisorbed thiol on the gold surface (thiolate), whereas the $\text{S}2\text{p}_{3/2}$ band with binding energy of 163.3 eV can be assigned to physisorbed thiol.³ Importantly, the S2p spectrum showed no evidence for oxidized and atomic sulfur, which typically appear at 167 and 161 eV, respectively.³ The strong incorporation of the free thiol molecules into the NP ligand shell was confirmed by ^1H NMR analysis that showed the lack of unbound thiol in the AuNP dispersions. The presence of physisorbed thiol indicates its production in the reaction of amine-capped AuNPs with xanthates. The fitting–deconvolution procedure for the Au4f region revealed the gold in three chemical states. The $\text{Au}4\text{f}_{7/2}$ bands with binding energies of 84.0 and 84.4 eV correspond to bulk (Au^0) and oxidized gold ($\text{Au}^{\delta+}$),

respectively.³ The presence of oxidized gold species indicates the formation of thiolate–gold bonding on the NP surface. The negatively shifted $\text{Au}4\text{f}_{7/2}$ band (green line, Figure 3) with a binding energy of 83.3 eV may be assigned to gold atoms in the topmost surface layer of the NPs³ or related to electron transfer from ligand or solid substrate to gold.

It is noted that a quite different behavior was observed recently for xanthates of general formula $\text{ROC}(\text{S})\text{S}^-\text{K}^+$, which cap metal NPs in a noncleavable manner, giving colloids of limited stability.¹⁸

To gain insight into the mechanism of formation of the thiolate assemblies from organic xanthates, we harnessed the NMR technique. Since the xanthate is cleaved by amine to thiocarbamate and thiol,¹⁹ we conjectured first that the excess dodecylamine remaining in the dispersion after the NP synthesis is solely responsible for generating thiol species and, subsequently, for the formation of a thiolate-protective layer around the NP. The cleavage of the xanthate group by the surface-bound amine seemed initially unfeasible.

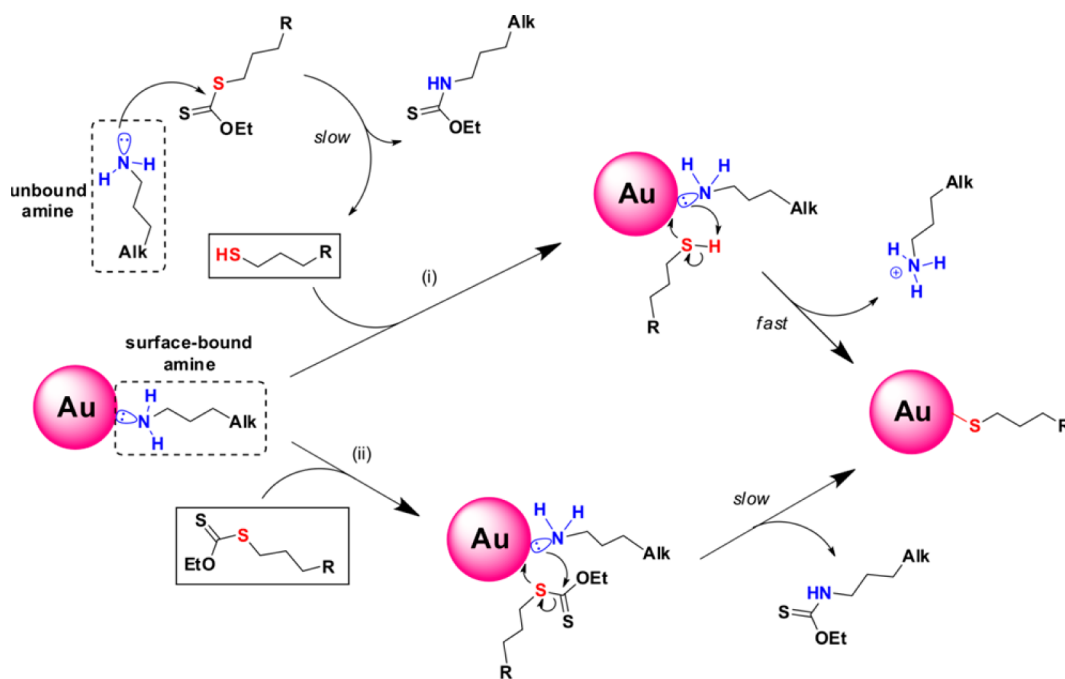


Figure 4. Plausible mechanism for thiolate–gold bond formation in the reaction of amine-capped NPs with xanthate. The reaction proceeds by two pathways simultaneously: (i) in the bulk phase, the unbound amine ligand cleaves the xanthate, generating thiol which next adsorbs to the NP surface forming a Au–S bond; (ii) cleavage of xanthate with formation of a Au–S bond occurs on the NP surface and is mediated by the surface-bound amine ligand. In both cases, the hydrogen generated upon the formation of a Au–S bond leaves the NP surface as a proton (protonated amine).

Presumably, the amine binds to the NP surface *via* Lewis acid sites (Au–Cl)²⁰ that should suppress its nucleophilic capability. Surprisingly, having performed a set of experiments, we ascertained that the formation of the gold–thiolate bond is mediated by the amine ligands coming from both the solution and the surface. A plausible mechanism for the formation of the Au–S bond is represented in Figure 4. In order to follow each pathway independently, we split the original reaction. We studied the interaction of xanthate with amine-capped AuNPs (surface-bound ligand) and bulk-phase amine (unbound ligand) in two separate model experiments. The changes that occurred in both processes were monitored using ¹H NMR spectroscopy. In the reaction of unbound amine with xanthate, the molar ratio of reagents was adjusted so that it was in the original reaction. In the second experiment, due to a low content of surface-bound amine on a single NP, we had to increase a total concentration of the amine-capped NPs to facilitate quantifying the reaction progression. The concentration of xanthate in both experiments left the same, which enabled the comparison of the two pathways. We found that the rate of xanthate cleavage by the amine-capped NPs was faster than that by the bulk-phase amine, despite the fact that the concentration of the unbound amine exceeded 10-fold that bound to the NP surface. This result suggests that the cleavage of xanthate by the amine-capped NPs is rather a surface-mediated process. The amount of thiolate generated by the surface-bound amine,

however, is not sufficient to fully cover the NP surface (*vide infra*). This means that the generation of thiol by an external (unbound) amine is necessary to complete the formation of a thiolate monolayer on the NP surface. Using the kinetic data of xanthate cleavage by unbound and surface-bound amine, we estimated that the formation of the thiolate monolayer is completed within 2 h. However, to be sure that a well-ordered structure of monolayer was formed, a prolonged reaction time (24 h) was typically applied for the preparation of thiolate-protected AuNPs shown in Figures 1 and 7.

When studying the pathway (i) (Figure 4), that is, the reaction of the thiol with the amine-capped AuNPs, we found that the formation of the thiolate monolayer proceeds instantly and is accompanied by the release of the amine in a protonated form. This finding indicates that the thiol, while adsorbing to the NP surface, leaves hydrogen as a proton. Our result differs from those reported recently where the scission of the S–H bond led to the formation of molecular hydrogen.^{11–13} The differences in hydrogen behavior can be caused by a surface composition of AuNPs and local chemical environment. A slow kinetics of xanthate cleavage by the amine-capped NPs (pathway (ii), Figure 4) allowed us to monitor the formation of thiolate monolayer and hence the fate of hydrogen in “slow motion”. It was found that only *ca.* 33% of the surface-bound amine undergoes the reaction with xanthate that consequently leads to partial coverage of the NP surface with thiolate ligands. No release of

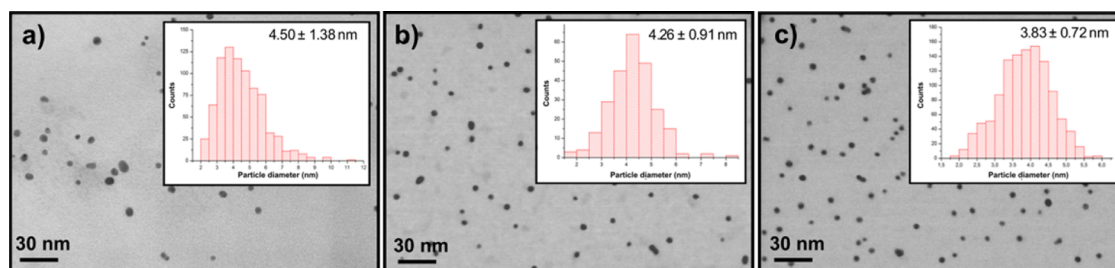


Figure 5. STEM micrographs of amine-capped AuNPs (a) and thiolate-protected AuNPs generated from the xanthate 2 (c) and its thiol analogue (b). The insets show the average diameter and size distributions of the AuNPs.

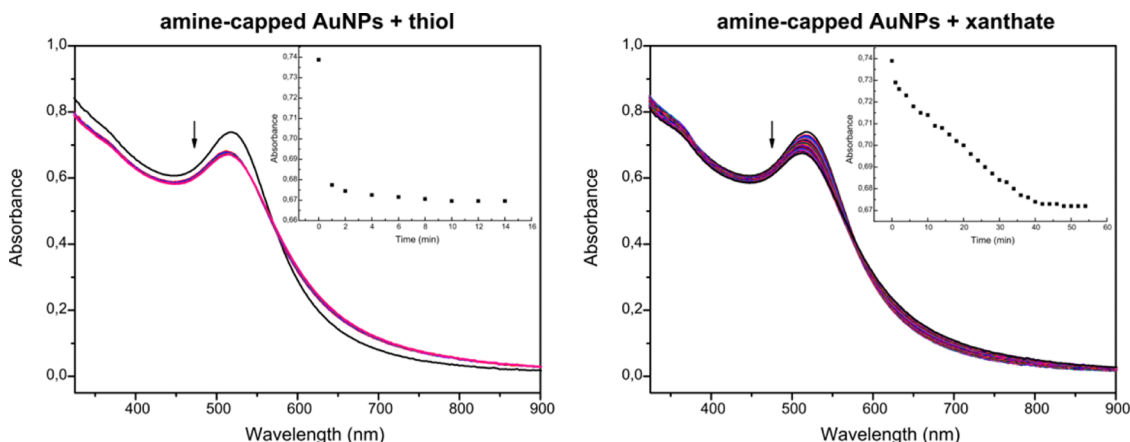


Figure 6. Time-resolved UV–vis spectra of the reaction of amine-capped AuNPs with xanthate 2 and its thiol analogue. The insets show the time evolution of absorbance at 518 nm (λ_{max} for the amine-capped AuNPs).

amine ligands was observed at this stage. After the cleavage reaction ceased, the NPs aggregated (most likely due to incomplete thiolate coverage on the surface) and released the amine ligands (protonated and nonprotonated ones) into the solution. Although we were not able to unravel the origin of ligand release, the obtained data set enabled us to draw the following important conclusions: The first is that the protons, after the thiolate bond is created, accumulate in the ligand shell by protonating the surrounding amine ligands. Since the protonated amine forms a weak bonding with the NP surface,²⁰ the release of amine ligands at the initial stage of formation of the thiolate monolayer was not observed. Second, the protonation of amine leads to the loss of its nucleophilic properties. This accounts for the fact that only a part of surface-bound amine is able to cleave the xanthate molecules. More details on the NMR studies are presented in the Supporting Information.

Finally, the transformation of amine-capped AuNPs into thiolate-protected AuNPs was examined using scanning transmission electron microscopy (STEM) and ultraviolet–visible (UV–vis) spectroscopy. STEM analysis revealed that NPs, after treatment with xanthate or thiol, have become more monodisperse and their mean core size decreased. The STEM micrographs and corresponding statistical analysis are provided in Figure 5. The amine-capped AuNPs had an average diameter of 4.50 nm (with dispersity $\sigma = 31\%$). In

contrast, the thiolate-protected AuNPs had average diameters of 4.26 nm ($\sigma = 21\%$) for thiol-derived particles and 3.83 nm ($\sigma = 19\%$) for the particles derived from the xanthate. The observed decline of NP mean size with simultaneous improvement of monodispersity can be rationalized by the thiol etching of the NP surface.²¹

The UV–vis study of the reaction of the amine-capped AuNPs with xanthate and thiol has shown the decrease of absorbance intensity of the surface plasmon resonance band that mostly is related to the formation of NP agglomerates as evidenced by visual observation (Figure 6). The degree of the agglomeration can be roughly estimated from the intensity decrease plot of absorbance *versus* time (see insets, Figure 6), affording the similar value of about 9% for both xanthate and thiol. The agglomeration of the NPs resulted probably from the inhomogeneous ligand coverage in the course of the thiolate monolayer formation when different types of ligands are present on the NP surface. Hence, the agglomeration process can serve as a measure of the reaction progress of the formation of the thiolate monolayer. Indeed, the agglomeration time frame (see insets, Figure 6) coincides well with that of the thiolate monolayer formation estimated on the basis of ¹H NMR analysis.

Thanks to xanthate approach, we can introduce into the NP ligand shell the functionalities which are

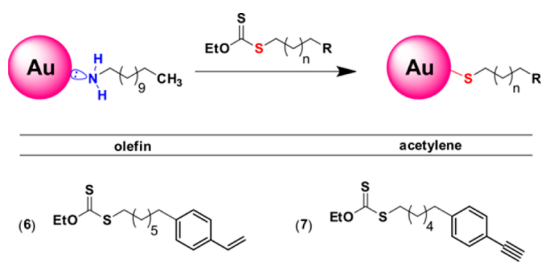


Figure 7. Introduction of thiol-sensitive unsaturated C–C bond functionalities into a AuNP ligand shell using the xanthate approach.

sensitive to thiol group. We envisioned that a gradual generation of thiol (thiolate), which instantly adsorbs to the NP surface, would prevent the self-reaction of functionalized thiol. In the present study, we explored the molecules incorporating unsaturated C–C bonds. The presence of olefin or acetylene groups can offer powerful tools for performing chemical transformations on the NP ligand shell under mild conditions, which is particularly important for environment-sensitive self-assembled and biological systems. The possible chemical toolkit for such transformations covers recently developed olefin/enyne metathesis²² and a family of click methodologies including thiol-ene,²³ thiol-yne,²⁴ and azide–alkyne reactions.²⁵ Normally, the olefins and acetylenes require external triggers, such as radical initiator or catalyst, to react with a thiol. However, the addition of a SH group to an unsaturated bond can also occur spontaneously. A considerable example of a thiol-sensitive group is a styrene moiety.²⁶ Noteworthy, the styrene moiety, in addition to aforementioned metathesis and click tools, also provides a versatile scaffold for polymerization chemistry. We found that the styrene-terminated thiol once isolated oligomerizes very quickly. Notably, we revealed that the thiol sensitivity problem becomes more universal and extends also to phenylacetylene functionality. Whether the addition of a thiol group to the unsaturated bonds occurs *via* a radical mechanism or Michael-type reaction is not clear but naturally limits the practical applicability of these important compounds. On the contrary, the molecules

protected with a xanthate group show no sign of decomposition upon storage for over 1 year. Employing the xanthate approach, we were able to readily introduce the styrene and phenylacetylene moieties into the NP ligand shell (Figure 7). Importantly, the NMR analysis has shown no traces of oligomerization products in the protective layer of modified NPs.

Finally, we note that the xanthate chemistry is not only limited to AuNPs but also can be applied for other NP systems. To demonstrate this, we successfully functionalized the amine-capped CdSe/ZnS quantum dots with a thiol-sensitive styrene group. The structure of modified NPs was confirmed on the basis of NMR analysis.

CONCLUSIONS

In summary, we discovered that the xanthate molecules, when brought into contact with amine-capped AuNPs, have been deposited as thiolate ligands on the NP surface. The formation of thiolate assemblies was unambiguously corroborated by NMR and XPS analyses. The mechanism underlying this process was elucidated from tracking the reaction progress using NMR spectroscopy. The complementary kinetic data were obtained using UV–vis spectroscopy. The information on the change of NP size during the transformation was provided by STEM microscopy. On the basis of the discovered phenomenon, we have developed a versatile “thiol-free” method that enables decoration of metal and semiconductor NPs with a variety of functional groups. Of particular importance and practical potential of the elaborated approach is the possibility to integrate the thiol-sensitive functionalities into the NP ligand shell that has been successfully demonstrated for styrene and phenylacetylene moieties. Moreover, the study on the reaction mechanism revealed that hydrogen upon chemisorption of thiol to the gold surface is released as a proton. This finding brings an unexpected twist to the current understanding of gold–thiol interaction. The issue that might seem to be already solved requires a thorough re-examination.

EXPERIMENTAL SECTION

Materials and Instrumentation. Chemicals and materials were purchased as reagent grade from commercial suppliers and used without further purification. The solvents used were of analytical grade quality. DDA-capped AuNPs with a core size of about 5 nm were prepared according to the literature procedure.¹⁴

Column chromatography was performed using Merck silica gel 60 (230–400 mesh ASTM). TLC was performed by using Merck silica gel 60 F₂₅₄ (0.2 mm) on alumina plates. NMR spectra were recorded on a Varian (400 MHz) instrument. The chemical shifts (δ) are given in parts per million relative to TMS, coupling constants (J) are in hertz. MS spectra were recorded on a LCT (TOF) spectrometer. XPS spectra were recorded on PHI 5000 VersaProbe X-ray photoelectron spectrometer using an Al K α X-ray source. STEM images were recorded on Hitachi S5500

instrument equipped with DuoStem detector. UV–vis spectra were recorded on Thermo Scientific Evolution 201 spectrophotometer.

Synthesis of Xanthate 2. Solid potassium ethyl xanthate (1.2 equiv, 6 mmol, 0.96 g) was added to a solution of 11-bromo-1-undecene (1.0 equiv, 5 mmol, 1.17 g) in acetone (15 mL) at room temperature and stirred for 6 h. The reaction mixture was passed through a short pad of silica to remove the inorganic material. After that, the solvent was evaporated and the residue was purified by column chromatography (hexanes/EtOAc 19:1) to give the product as a colorless oil (1.07 g, 78%). ¹H NMR (400 MHz, CDCl₃): δ 5.80 (ddt, J = 17.0, 10.2, 6.7 Hz, 1H), 5.04–4.86 (m, 2H), 4.64 (q, J = 7.1 Hz, 2H), 3.10 (t, J = 7.4 Hz, 2H), 2.03 (m, 2H), 1.68 (quint, J = 7.4 Hz, 2H), 1.41 (t, J = 7.1 Hz, 3H), 1.46–1.18 (m, 12H). ¹³C NMR (100 MHz, CDCl₃): δ 215.2, 139.1, 114.1, 69.7, 35.9, 33.7, 29.3, 29.3,

29.0, 28.9, 28.8, 28.3, 13.8. HRMS (ESI): m/z calcd for $C_{14}H_{26}OS_2Na$ 297.1323 [M + Na], found 297.1329.

Preparation of Thiolate-Protected AuNPs. A solution of xanthate **2** (1 equiv, 0.2 mmol, 54 mg) in toluene (1 mL) was added to the dispersion of DDA-capped AuNPs (26 g, 0.2 mmol in terms of gold atoms), and the resulting mixture was stirred at room temperature for 24 h. The obtained NPs were precipitated with methanol and collected by centrifugation (3000–5000 rpm). The NP precipitate was dispersed in a minimal amount of *n*-hexane, precipitated with methanol, and collected by centrifugation. The redispersion–precipitation procedure was repeated six times to remove organic contaminants from the NPs.

For the preparation of the thiolate-protected NPs from thiol, the same procedure was applied.

NP Characterization by NMR. The purified NPs (~0.1 mmol in terms of gold atoms) were dissolved in $CDCl_3$, and 1H NMR spectrum was recorded. After that, the ligands were desorbed from the surface of NPs by adding a few crystals of iodine directly to the NMR tube, and the spectrum was re-recorded.

NP Characterization by XPS. The purified NPs (~0.1 mmol in terms of gold atoms) were dissolved in a small amount of *n*-hexane and filtered through a short pad of cotton. The concentrated NP solutions were drop-cast onto clean silicon wafers (five depositions). Each droplet was allowed time to dry between depositions. The spectra were recorded with a pass energy of 23.5 eV and a photoelectron takeoff angle of 45° from the surface. The base pressure in the chamber during measurements was 1×10^{-9} Torr, and the spectra were collected from a spot of $250 \times 250 \mu m$ at room temperature.

NP Characterization by STEM. The purified NPs were dissolved in chloroform and next drop-cast on a copper grid, and STEM images were recorded at an accelerating voltage of 30 kV. (The purified DDA-capped AuNPs were obtained by the precipitation from the original AuNP dispersion using methanol followed by extensive methanol rinsing.)

UV–Vis Experiments. The original AuNP dispersion (100 mg, ~0.77 μmol in terms of gold atoms) was added to each cuvette and diluted with 3 mL of a stock solution. The stock solution was prepared by dissolving DDA (1.00 g) and dimethyldidodecylammonium bromide (1.13 g) in toluene (40 mL). The use of the stock solution aimed to maintain the original concentration of amine and surfactant in the AuNP dispersion after its dilution. The solutions of thiol and xanthate (77 mM in toluene, 10 μL) were added to each cuvette, and the UV–vis spectra were recorded in 1 and 2 min intervals.

Conflict of Interest: The authors declare no competing financial interest.

Acknowledgment. This project was funded by National Science Center (Grant DEC-2011/01/D/ST5/03518). M. Fialkowski and M. Michalak are gratefully acknowledged for critical reading of the manuscript and valuable comments.

Supporting Information Available: Details on synthesis and characterization of all ligands and NPs, mechanistic studies. This material is available free of charge via the Internet at <http://pubs.acs.org>.

REFERENCES AND NOTES

- Hakkinen, H. The Gold–Sulfur Interface at the Nanoscale. *Nat. Chem.* **2012**, *4*, 443–455.
- Love, J. C.; Estroff, L. A.; Kriebel, J. K.; Nuzzo, R. G.; Whitesides, G. M. Self-Assembled Monolayers of Thiolates on Metals as a Form of Nanotechnology. *Chem. Rev.* **2005**, *105*, 1103–1170.
- Vericat, C.; Vela, M. E.; Benitez, G.; Carro, P.; Salvarezza, R. C. Self-Assembled Monolayers of Thiols and Dithiols on Gold: New Challenges for a Well-Known System. *Chem. Soc. Rev.* **2010**, *39*, 1805–1834.
- Jans, H.; Huo, Q. Gold Nanoparticle-Enabled Biological and Chemical Detection and Analysis. *Chem. Soc. Rev.* **2012**, *41*, 2849–2866.
- Saha, K.; Agasti, S. S.; Kim, C.; Li, X.; Rotello, V. M. Gold Nanoparticles in Chemical and Biological Sensing. *Chem. Rev.* **2012**, *112*, 2739–2779.

- Giljohann, D. A.; Seferos, D. S.; Daniel, W. L.; Massich, M. D.; Patel, P. C.; Mirkin, C. A. Gold Nanoparticles for Biology and Medicine. *Angew. Chem., Int. Ed.* **2010**, *49*, 3280–3294.
- Shon, Y.-S.; Gross, S. M.; Dawson, B.; Porter, M.; Murray, R. W. Alkanethiolate-Protected Gold Clusters Generated from Sodium S-Dodecylthiosulfate (Bunte Salts). *Langmuir* **2000**, *16*, 6555–6561.
- Zhang, S.; Leem, G.; Lee, T. R. Monolayer-Protected Gold Nanoparticles Prepared Using Long-Chain Alkanethioacetates. *Langmuir* **2009**, *25*, 13855–13860.
- Porter, L. A.; Ji, D.; Westcott, S. L.; Graupe, M.; Czernuszewicz, R. S.; Halas, N. J.; Lee, T. R. Gold and Silver Nanoparticles Functionalized by the Adsorption of Dialkyl Disulfides. *Langmuir* **1998**, *14*, 7378–7386.
- Zhu, J.; Ganton, M. D.; Kerr, M. A.; Workentin, M. S. Chemical Modification of Monolayer-Protected Gold Nanoparticles Using Hyperbaric Conditions. *J. Am. Chem. Soc.* **2007**, *129*, 4904–4905.
- Kankate, L.; Turchanin, A.; Götzhäuser, A. On the Release of Hydrogen from the S–H Groups in the Formation of Self-Assembled Monolayers of Thiols. *Langmuir* **2009**, *25*, 10435–10438.
- Petroski, J.; Chou, M.; Creutz, C. The Coordination Chemistry of Gold Surfaces: Formation and Far-Infrared Spectra of Alkanethiolate-Capped Gold Nanoparticles. *J. Organomet. Chem.* **2009**, *694*, 1138–1143.
- Matthiesen, J. E.; Jose, D.; Sorensen, C. M.; Klabunde, K. J. Loss of Hydrogen upon Exposure of Thiol to Gold Clusters at Low Temperature. *J. Am. Chem. Soc.* **2012**, *134*, 9376–9379.
- Jana, N. R.; Peng, X. Single-Phase and Gram-Scale Routes toward Nearly Monodisperse Au and Other Noble Metal Nanocrystals. *J. Am. Chem. Soc.* **2003**, *125*, 14280–14281.
- Kalsin, A. M.; Fialkowski, M.; Paszewski, M.; Smoukov, S. K.; Bishop, K. J. M.; Grzybowski, B. A. Electrostatic Self-Assembly of Binary Nanoparticle Crystals with a Diamond-like Lattice. *Science* **2006**, *312*, 420–424.
- Sashuk, V.; Holyst, R.; Wojciechowski, T.; Fialkowski, M. Close-Packed Monolayers of Charged Janus-Type Nanoparticles at the Air–Water Interface. *J. Colloid Interface Sci.* **2012**, *375*, 180–186.
- Sashuk, V.; Holyst, R.; Wojciechowski, T.; Górecka, E.; Fialkowski, M. Autonomous Self-Assembly of Ionic Nanoparticles into Hexagonally Close-Packed Lattices at a Planar Oil–Water Interface. *Chem.—Eur. J.* **2012**, *18*, 2235–2238.
- Tzhayik, O.; Sawant, P.; Efrima, S.; Kovalev, E.; Klug, J. T. Xanthate Capping of Silver, Copper, and Gold Colloids. *Langmuir* **2002**, *18*, 3364–3369.
- Kraatz, U. In *Methoden der Organischen Chemie (Houben-Weyl)*; Hagemann, H., Ed.; Georg Thieme Verlag: Stuttgart, New York, 1983; Vol. E4, p 439.
- Kumar, A.; Mandal, S.; Pasricha, R.; Mandale, A. B.; Sastry, M. Investigation into the Interaction between Surface-Bound Alkylamines and Gold Nanoparticles. *Langmuir* **2003**, *19*, 6277–6282.
- Qian, H.; Zhu, M.; Lanni, E.; Zhu, Y.; Bier, M. E.; Jin, R. Conversion of Polydisperse Au Nanoparticles into Monodisperse Au₂₅ Nanorods and Nanospheres. *J. Phys. Chem. C* **2009**, *113*, 17599–17603.
- Hoveyda, A. H.; Zhugralin, A. R. The Remarkable Metal-Catalysed Olefin Metathesis Reaction. *Nature* **2007**, *450*, 243–251.
- Hoyle, C. E.; Bowman, C. N. Thiol-Ene Click Chemistry. *Angew. Chem., Int. Ed.* **2010**, *49*, 1540–1573.
- Hoogenboom, R. Thiol-Yne Chemistry: A Powerful Tool for Creating Highly Functional Materials. *Angew. Chem., Int. Ed.* **2010**, *49*, 3415–3417.
- Meldal, M.; Tornøe, C. W. Cu-Catalyzed Azide-Alkyne Cycloaddition. *Chem. Rev.* **2008**, *108*, 2952–3015.
- Todd Banner, L.; Tekobo, S.; Garay, F.; Clayton, B. T.; Thomas, Z. P.; Lindner, E.; Richter, A. G.; Pinkhassik, E. Self-Limiting Robust Surface-Grafted Organic Nanofilms. *Chem. Mater.* **2010**, *22*, 2248–2254.